

On Slepian Series Expansion For Digitized Signals

Journal:	<i>Applicable Analysis</i>
Manuscript ID:	GAPA-2010-0230
Manuscript Type:	Original Paper
Date Submitted by the Author:	23-Jun-2010
Complete List of Authors:	Shen, Xiaoping; Ohio University, Mathematics Saito, Naoki; University of California-Davis, Mathematics
Keywords:	Slepian (PSWF) series, othorgonal expansion, bandlimited signals
Note: The following files were submitted by the author for peer review, but cannot be converted to PDF. You must view these files (e.g. movies) online.	
SHEN-SAITO06232010.rar	



RESEARCH ARTICLE

*On Slepian Series Expansion For Digitized Signals*Xiaoping Shen^{a*} and Naoki Saito^b^a*Department of Mathematics, Ohio University, Athens, OH 45701, USA;*^b*Department of Mathematics, University of California, Davis, CA 95616, USA**(Version 1.0 released June 2010)*

Prolate spheroidal wave functions (Slepian functions) are special functions that are most localized in both spatial and frequency domain, simultaneously. They lead to the optimal solution of the concentration problem once posed by Claude E. Shannon. This fact was unraveled by David Slepian and his collaborators at Bell Lab in 1960s. Since then this system has shown promise for many applications in engineering and some other areas. Unlike usual orthogonal polynomials or trigonometric systems, Slepian functions possess peculiar properties, such as, dual orthogonality, duality of time-frequency representation, and multiscale structure, to name a few. This paper is devoted to the study of Slepian series for digitized functions in the Paley-Wiener space and beyond. We shall give the convergence analysis of the expansion coefficients and explore their properties by numerical experiments. We conclude the paper by discussing problems raised in such expansions used in the practice when only the discrete data are available and contaminated by noise.

Keyword Slepian (PSWF) series, concentration problem, orthogonal expansion, bandlimited signals, Paley-Wiener space, Gibbs phenomenon.

Mathematics Subject Classification Primary 42C40, 65T60; Secondary 33E10, 42C05, 94A11, 94A12.

1. Introduction

The theoretical aspects of using prolate spheroidal wave functions (PSWFs) as the solution of energy concentration problem have been known for over forty years. Extensive studies of PSWFs in the context of communication theory were done at Bell Laboratory. Much of the research was performed by D. Slepian, H. J. Landau and H. O. Pollak and their colleagues (See [11], [12], [23] and [22]). Consequently, the PSWFs have come to be known as Slepian functions affectionately in engineering community. Since then many applications have been developed in different areas such as in telecommunication, signal/image processing to attack problems raised in filter design (achieve minimal side lobes), minimizing inter symbol interference (ISI), prediction/extrapolation envelopes of wireless signals, and MRI medical image processing [3], [18], [33], [34]. However, most of these applications are based on the discrete prolate spheroidal wave functions (DPSWFs) [20] or finite prolate spheroidal wave function (FPSWFs) [33], [34]. Their publicity has been promoted by the program DPSS in the well known software MATLAB[®]. This is because the actual evaluation of specific PSWFs in closed form presents formidable difficulties and their implementations were exceedingly expensive [6], unfortunately. Many efforts have been made to compute these functions. Some classic methods to

*Corresponding author. Email: shen@math.ohiou.edu

compute function values can be found in [2], [4] and [7]. In 1970s, Naval Research Laboratory (Washington, DC) has made significant contributions to the numerical computations of PSWFs by their projects [8], [5], [9], [27], and [28]. Most of the applications related to PSWFs rely on the this data sources. Basically, numerical methods used in these computations can be categorized as follows:

(1) Approximation by other special functions. These methods are usually using the Legendre polynomial in a finite interval and the Bessel functions on outside of the finite interval [37];

(2) Interpolation or sampling based method. These methods derive discrete values of PSWFs by solving a discrete optimization problem which is equivalent to the original concentration problem (a continuous optimization problem); and

(3) Iterative method. A numerical method based on asymptotic expansion developed by D. Slepian in [21]. This method is not as well-known as others.

The barriers limited by the human computing powers to unravel the mystery of the PSWFs are not as the same as before. Recently, the rapidly improved modern computational facilities and the advanced computational techniques such as generalized Gaussian quadrature [1], [36], have made it possible to develop less expensive applications in many areas, such as numerical solutions for partial differential equations (PDEs) or in medical image processing. Further, some multiscale systems based on these original Slepian functions, such as Slepian semi wavelets, periodic Slepian wavelets ([16], [17], [31], and [32]).

In this article, we report some numerical results from our investigation on the orthogonal expansion series using continuous Slepian functions. Some of the results are extracted from annual reports of grant ONR YIP N00014-00-1-0469. The paper is organized as follows: background materials, such as definitions and terminology, related to the discussion of PSWFs are introduced briefly in the next section. We then are able to introduce Slepian series and discuss its properties for some function classes in Section 3. In Section 4, we demonstrate the convergence properties for functions in three difference categories:

C1. functions in Paley-Wiener space (see definition below);

C2. functions are essentially bandlimited, functions; and

C3. functions that are piecewise analytic with jump discontinuities.

Finally, we give some remarks on further study at the close of the article.

2. Background

To begin with, we recall the following background materials.

2.1. Paley-Wiener space

Definition 2.1: (Fourier transform) Let $h(t) \in L^2(\mathbb{R})$ be an arbitrary function; then the Fourier transform of $h(t)$ is the function defined by the integral

$$\mathcal{F}[h](\omega) = \hat{h}(\omega) = \int_{-\infty}^{\infty} h(x) e^{-i\omega x} dx \quad (1)$$

for those values of f for which the integral exists. The inverse transform is given by

$$h(x) = \frac{1}{2\pi} \int_{-\infty}^{\infty} \widehat{h}(\omega) e^{-i\omega x} d\omega \tag{2}$$

Theorem 2.2: (Paley-Wiener) Assume that $h \in L^p(\mathbb{R})$ is analytic. If there are positive constants K and σ so that for all $z \in \mathbb{C}$

$$|h(z)| \leq K \exp(\sigma|z|), \tag{3}$$

then $\widehat{h} \in L^2(-\sigma, \sigma)$ and

$$h(z) = \int_{-\sigma}^{\sigma} \widehat{h}(x) \exp(-2\pi i x z) dx \tag{4}$$

(Paley-Wiener) Assume that $h \in L^p(\mathbb{R})$, $0 < p < \infty$ is analytic. If there are positive constants K and σ such that for all $z \in \mathbb{C}$,

$$|h(z)| \leq K e^{\sigma|z|}, \tag{5}$$

then $\widehat{h} \in L^2(-\sigma, \sigma)$ and

$$h(z) = \int_{-\sigma}^{\sigma} \widehat{h}(x) e^{-i2\pi x z} dx \tag{6}$$

A function satisfies (5) is said to be exponential type. A function satisfies (6) is said to be σ bandlimited.

The Paley-Wiener space belonging to $L^p(\mathbb{R})$, denote by \mathbf{B}_σ^p , is the space consists of all functions which satisfy Paley-Wiener Theorem. We summarized some related properties of Paley-Wiener spaces in the following proposition. Readers can find references in [25], [38].

From now on, we work with the case $p = 2$.

Definition 2.3: (Concentration index) Denote

$$\alpha^2(\tau, h) \equiv \frac{\int_{-\tau}^{\tau} |h(t)|^2 dt}{\int_{-\infty}^{\infty} |h(t)|^2 dt} \tag{7}$$

and

$$\beta^2(\sigma, h) \equiv \frac{\int_{-\sigma}^{\sigma} |\widehat{h}(w)|^2 dw}{\int_{-\infty}^{\infty} |\widehat{h}(w)|^2 dw} \tag{8}$$

We refer α as *time concentration index* and β *frequency concentration index* of signal h . Notice that for all functions in L^2 , $0 \leq \alpha^2(\tau, h), \beta^2(\sigma, h) \leq 1$. All σ -bandlimited functions satisfy $\beta^2(\sigma, h) = 1$, whereas timelimited functions satisfy $\alpha^2(\sigma, h) = 1$.

Definition 2.4: (ε - essential bandlimited functions) Let $h \in L^1(\mathbb{R})$. f is essential σ - bandlimited if it satisfies the property: for $\sigma > 0, \exists \varepsilon > 0$, (ε is dependent on h and σ) such that

$$\int_{-\sigma}^{\sigma} |\widehat{h}(w)|^2 dw < \varepsilon$$

It is worth mentioning that a function could be analytic but not of exponential type, while it could also be of exponential type but not analytic. Some examples are shown in Section 4.

2.2. Concentration problem and its solution

The Slepian functions (PSWFs) $\psi_{n,\sigma,\tau}(x)$ can be defined in number of different ways, for example,

1. as the eigenfunctions of an integral operator :

$$\int_{-\tau}^{\tau} \psi_{n,\sigma,\tau}(x) S\left(\frac{\sigma}{\pi}(t-x)\right) dx = \lambda_{n,\sigma,\tau} \psi_{n,\sigma,\tau}(t), \tag{9}$$

where $S(t) = \frac{\sin \pi t}{\pi t}$ is the sinc function.

2. as the eigenfunctions of a differential operator:

$$(\tau^2 - t^2) \frac{d^2 \psi_{n,\sigma,\tau}}{dt^2} - 2t \frac{d \psi_{n,\sigma,\tau}}{dt} - \sigma^2 t^2 \psi_{n,\sigma,\tau} = \mu_{n,\sigma,\tau} \psi_{n,\sigma,\tau}. \tag{10}$$

or

3. as the maximum energy concentration of a σ - bandlimited function on the interval $[-\tau, \tau]$; that is $\psi_{0,\sigma,\tau}$ is the function of total energy 1 ($= \|\psi_{0,\sigma,\tau}\|^2$) such that $\alpha^2(\tau, \psi_{0,\sigma,\tau})$ is maximized, $\psi_{1,\sigma,\tau}$ is the function with the maximum energy concentration among those functions orthogonal to $\psi_{0,\sigma,\tau}$, etc.

Still another characterization in terms of multiplication operators is possible and may be found in [29], while another integral eigenvalue problem also satisfied by the $\psi_{n,\sigma,\tau}$ is [13],

$$\int_{-\tau}^{\tau} \psi_{n,\sigma,\tau}(x) e^{i\sigma\omega x/\tau} dx = \gamma_{n,\sigma,\tau} \psi_{n,\sigma,\tau}(\omega). \tag{11}$$

The parameter τ comes from the interval of concentration and the parameter σ comes from the support of the Fourier transform . The time concentration indices for $\psi_{n,\sigma,\tau}(\omega)$ is $\alpha^2(\tau, \psi_{n,\sigma,\tau}) = \lambda_{n,\sigma,\tau}, n = 0, \dots,$

Figure 1 shows several of the PSWFs on the concentration interval $[-1, 1]$. The corresponding eigenvalues (concentration indices) are shown in Figure 2.

The concentration problem is to determine functions in \mathbf{B}_{σ}^2 with maximum time concentration index α on interval $[-\tau, \tau]$, they can be derived from the eigenvalue problem of the integral equation (9). Since the kernel is positive defined, its spectrum is discrete set and

$$1 > \lambda_{0,\sigma,\tau} \geq \lambda_{1,\sigma,\tau} \geq \dots \geq \lambda_{n,\sigma,\tau} \geq \dots > 0$$

with $\lim_{n \rightarrow \infty} \lambda_{n,\sigma,\tau} = 0$. The corresponding eigenfunctions, $\{\psi_{n,\sigma,\tau}(x)\}_{k=0}^{\infty}$ can be chosen to be real and orthogonal on $[-\tau, \tau]$. By using the left hand side of (9),

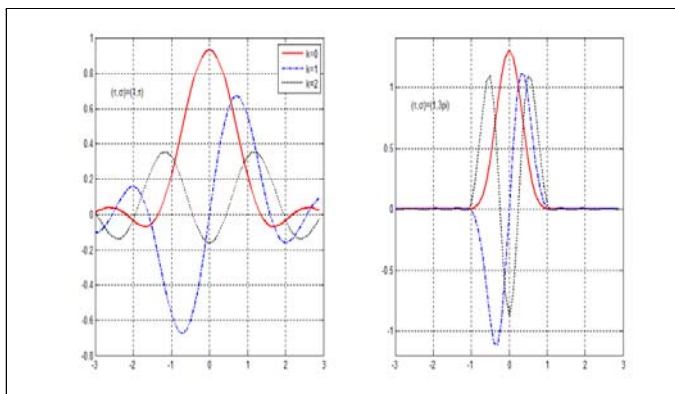


Figure 1. Slepian functions $\psi_{n,\sigma,\tau}$. Left panel: $(\tau, \sigma) = (1, \pi)$, $n = 0, 1, 2$. Right panel: $(\tau, \sigma) = (1, 3\pi)$, $n = 0, 1, 2$.

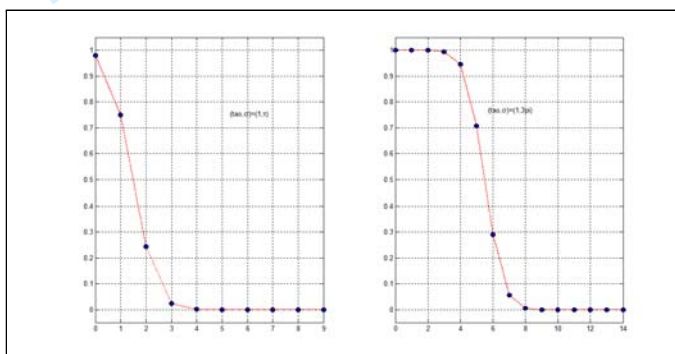


Figure 2. Associated eigenvalues $\lambda_{n,\sigma,\tau}$. Left panel: $(\tau, \sigma) = (1, \pi)$, $n = 0, 1, 2, \dots, 9$. Right panel: $(\tau, \sigma) = (1, 3\pi)$, $n = 0, 1, 2, \dots, 14$.

we could further extend the definition of $\psi_{n,\sigma,\tau}$ to outside of $[-\tau, \tau]$ (see [19] as follows:

$$\int_{-\tau}^{\tau} S\left(\frac{\sigma}{\pi}(x-y)\right) \psi_{n,\sigma,\tau}(y) dy = \lambda_{n,\sigma,\tau} \psi_{n,\sigma,\tau}(x), \quad |x| > \tau. \quad (12)$$

Unfortunately, analytic solutions to (9) or (10) are not possible. However, several approaches have been developed to evaluate PSWFs numerically.

2.3. Related properties of prolate spheroidal wave functions

Let $\{\psi_{n,\sigma,\tau}(x)\}$ be a set of eigenfunctions of (9), then we have the following properties:

- (1) **Double orthogonality.**

$$\int_{-\tau}^{\tau} \psi_{n,\sigma,\tau}(x) \psi_{m,\sigma,\tau}(x) dx = \lambda_{n,\sigma,\tau} \delta_{nm}, \quad (13)$$

$$\int_{-\infty}^{\infty} \psi_{n,\sigma,\tau}(x) \psi_{m,\sigma,\tau}(x) dx = \delta_{nm}. \quad (14)$$

- (2) **Duality in time-frequency domain.** The Fourier transform of $\psi_{n,\sigma,\tau}$ is

given by

$$\widehat{\psi}_{n,\sigma,\tau}(\omega) = (-1)^n \sqrt{\frac{2\pi\tau}{\sigma\lambda_{n,\sigma,\tau}}} \varphi_{n,\sigma,\tau}\left(\frac{\tau\omega}{\sigma}\right) \chi_{\sigma}(\omega). \quad (15)$$

Hence, we also have

$$\psi_{n,\sigma,\tau}(x) = (-1)^n \sqrt{\frac{2\pi\tau}{\sigma\lambda_{n,\sigma,\tau}}} \frac{1}{2\sigma} \int_{-\sigma}^{\sigma} \psi_{n,\sigma,\tau}\left(\frac{\tau\omega}{\sigma}\right) e^{i\omega t} d\omega \quad (16)$$

Figure 3 shows a time and frequency pair of a Slepian function.

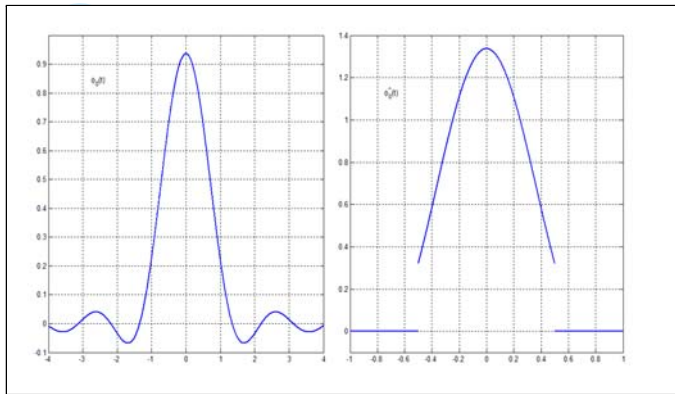


Figure 3. Slepian function $\psi_{0,\pi,1}(x)$ (left panel) and its Fourier transform $\widehat{\psi}_{0,\pi,1}(\omega)$ (right panel).

- (1) **Completeness.** $\{\psi_{n,\sigma,\tau}(x)\}$ are complete in space $L^2(-\tau, \tau)$.
- (2) **Step function behavior.** The sequence $\{\lambda_{n,\sigma,\tau}\}$ consists of approximately $2\sigma\tau$ eigenvalues that are close to 1, and about $\log \sigma\tau$ eigenvalues which decay exponentially to zero, as $n \rightarrow \infty$ (see Figure 2).

3. Slepian series

Let $h(x) \in L^2(-1, 1)$. We write formally,

$$\begin{aligned} h(x) &= \sum_{k=0}^{\infty} h_{k,\sigma,\tau} \psi_{k,\sigma,\tau}(x) = \sum_{k=0}^{N-1} h_{k,\sigma,\tau} \psi_{k,\sigma,\tau}(x) + \sum_{k=N}^{\infty} h_{k,\sigma,\tau} \psi_{k,\sigma,\tau}(x) \quad (17) \\ &= \mathbf{P}_{N,\sigma,\tau}[h](x) + \mathbf{E}_{N,\sigma,\tau}[h](x) \end{aligned}$$

where $\mathbf{P}_N : L^2[-1, 1] \rightarrow E_{\lambda_0} \oplus E_{\lambda_1} \oplus \dots \oplus E_{\lambda_N}$, is the projection operator. $\mathbf{E}_N[h](x) = \sum_{k=N}^{\infty} h_{k,\sigma,\tau} \psi_{k,\sigma,\tau}(x)$ is the remainder. Notice that the expansion coefficient $h_{k,\sigma,\tau}$ are dependent on parameters σ and τ . However, for simplicity, we will omit the indices σ, τ of the expansion coefficients.

To determine coefficients h_k , we could use either the finite orthogonality (13) or infinite orthogonality 14 of $\psi_{k,\sigma,\tau}$. We will assume the availability of function

values only within the interval $[-\tau, \tau]$ and use (13) to get,

$$h_{k,\sigma,\tau} = (h, \psi_{k,\sigma,\tau}) = \frac{1}{\lambda_{k,\sigma,\tau}} \int_{-\tau}^{\tau} h(x) \psi_{k,\sigma,\tau}(x) dx. \tag{18}$$

Notice that, in such setting, the series (17) can be used for extrapolation purpose. We first discuss the convergence rates of the expansion coefficients analytically, and then devote all our effort to explore their properties numerical properties.

3.1. The convergence of the Slepian series

The differential equation (10) defining $\psi_{n,\sigma,\tau}$ can be rewritten as [2],

$$((1-t^2)\psi'_{n,\sigma,\tau})' + (\mu_n - c^2t^2)\psi_{n,\sigma,\tau} = \mathbf{P}\psi_{n,\sigma,\tau} + \mu_n = 0,$$

where $c = \sigma\tau$ and the Sturm-Liouville differential operator \mathbf{P} is self adjoint. The eigenvalues $\mu_n = O(n^2)$ as $n \rightarrow \infty$. Using integration by parts, the expansion coefficients of a function $f \in C^{2m}[-1, 1]$ can be written as

$$\begin{aligned} f_n &= \langle f, \psi_{n,\sigma,\tau} \rangle = (\mu_n)^{-m} \langle f, \mathbf{P}^m \psi_{n,\sigma,\tau} \rangle, \\ &= (\mu_n)^{-m} \langle \mathbf{P}^m f, \psi_{n,\sigma,\tau} \rangle = (\mu_n)^{-m} b_n, \end{aligned}$$

where b_n are the coefficients of the continuous function $\mathbf{P}^m f$. Hence we have

$$f_n = o(n^{-2m}).$$

Another approach involves the integral operator satisfied by the $\psi_{n,\sigma,\tau}$:

$$\lambda_{n,\sigma,\tau}(t) = \int_{-\tau}^{\tau} e^{ictx} \psi_{n,\sigma,\tau}(x) dx.$$

We now let $f = K^m g$, where $g \in L^2[-\tau, \tau]$, and K is the integral operator

$$(Kg)(t) \equiv \int_{-\tau}^{\tau} e^{-ictx} g(x) dx.$$

Then the coefficients are given by

$$\begin{aligned} f_n &= \langle f, \psi_{n,\sigma,\tau} \rangle = \langle K^m g, \psi_{n,\sigma,\tau} \rangle \\ &= \langle g, (K^m)^* \psi_{n,\sigma,\tau} \rangle = \overline{\lambda_n^m} \langle g, \psi_{n,\sigma,\tau} \rangle, \end{aligned} \tag{19}$$

where ‘*’ means conjugate. The last equality in above equation shows the coefficient converges to 0 very rapidly. These discussions lead to the following convergence theorem:

Theorem 3.1: Let $\psi_{k,\sigma,\tau}$ normalized by $\|\psi_{k,\sigma,\tau}\|_{L^2(-\tau,\tau)}^2 = 1$, $k = 0, 1, \dots$, be the k th PSWF belonging the Paley-Wiener space \mathbf{B}_σ and concentrated on $[-\tau, \tau]$. Let $f_{k,\sigma,\tau} = \langle f, \psi_{k,\sigma,\tau} \rangle$, i.e., the is the k th expansion coefficient of f with respect to the Slepian sequence. If $f \in L^2(\mathbb{R})$, we have

- (i) $f_{n,\sigma,\tau} = O(\exp(-\alpha(\sigma, \tau)n))$, if $f \in \mathbf{B}_\sigma$, where $\alpha = \alpha(\sigma, \tau)$ is independent of n ;

- (ii) $f_{n,\sigma,\tau} = o(n^{-2m})$, if $f \in C^{2m}(R)$;
- (iii) $\sum_{k=0}^{\infty} f_k \psi_{k,\sigma,\tau}(x)$ convergence uniformly on $[-\tau, \tau]$ if f satisfies the Lipschitz condition.

3.2. Computation of expansion coefficients

In the past, the numerical properties of the coefficients of Slepian series were rarely found in the literature. This may be due to the difficulties in numerically computing Slepian functions themselves. Clearly, to compute expansion coefficients (18), we have to adopt numerical methods. These involve methods used to compute the eigensystem $\{\lambda_{k,\sigma,\tau}, \psi_{k,\sigma,\tau}\}$ and numerical integration technique.

We will employ the Generalized Gaussian quadrature developed in [36] to compute the eigen system. After that, we use the same quadrature to calculate the expansion coefficients. We recall,

Definition 3.2: A quadrature formula will be referred as a (generalized) Gaussian quadrature with respect to a set of $2n$ polynomials:

$$\psi_1, \dots, \psi_{2n} : [a, b] \mapsto \mathbb{R}$$

and a weight function (non negative integrable):

$$w : [a, b] \mapsto \mathbb{R}^+$$

if it consists of n weights and nodes and integrates the function ψ_i exactly with the weight function w for all $i = 1, \dots, 2n$. The weights and nodes of a Gaussian quadrature will be referred as Gaussian weights and nodes, respectively..

Notice that if functions ψ_i are polynomials, the quadrature is a Gaussian quadrature. We will use the generalized Gaussian quadratures based on Slepian functions $\{\psi_{n,\sigma,\tau}\}$ with weight function $w = 1$ [36]. A generalized Gaussian quadrature has the format:

$$I[\omega, h; n] = \sum_{k=1}^n \omega_k h(x_k)$$

and satisfies

$$I[W, \psi_i; n] = \int_a^b W(x) \psi_i(x) dx, \quad i = 1, \dots, 2n \tag{20}$$

To emphasize the bandwidth σ and the PSWFs in using, we denote such a n - node quadrature by

$$I[\omega, h; n, \sigma] = \sum_{k=1}^n \omega_k h(x_k).$$

Notice that weight coefficients $\{\omega_k\}$ and notes $\{x_k\}$ are dependent on $c = \sigma\tau$, we suppress it for simplicity. The error analysis of this generalized Gaussian Quadrature is summarized as in the following:

([36], [35]). Suppose that the n -point quadrature with nodes $x_1, x_2, \dots, x_n \in (-1, 1)$ and weights w_1, w_2, \dots, w_n integrate exactly each of the functions $\psi_0^c, \psi_1^c, \dots, \psi_{m-1}^c$,

so that

$$\sum_{k=1}^n w_k \psi_j^c(x_k) = \int_{-1}^1 \psi_j^c(x) dx, \quad j = 1, \dots, m-1.$$

Then, for all $a \in (-1, 1)$ and real positive c ,

$$\left| \sum_{k=1}^n w_k e^{icax_k} - \int_a^b e^{icax} dx \right| \leq \epsilon$$

Theorem 3.3: ([35]) For a bandlimited function $g : [-1, 1] \rightarrow \mathbb{C}$ given by the formula

$$g(x) = \int_{-1}^1 G(t) e^{icxt} dt$$

with function $G : [-1, 1] \rightarrow \mathbb{C}$, the error of using generalized Gaussian quadrature is bounded by the formula

$$\left| \sum_{k=1}^n w_k g(x_k) - \int_{-1}^1 g(x) dx \right| \leq \epsilon \|G\|_{L_2[-1,1]} \quad (21)$$

where ϵ is as in the Lemma 3.

Now we take a close look of the inner products in the orthogonal expansion. We first observe that $h(x)\psi_{k,\sigma,\tau}(x) \in \mathbf{B}_{2\sigma}$ if $h \in \mathbf{B}_\sigma$. This can be seen from the Fourier transform of $h(x)\psi_{k,\sigma,\tau}(x)$, which is given by

$$\begin{aligned} & \int_{-\infty}^{\infty} h(x)\psi_{k,\sigma,\tau}(x)e^{-iwx} dx \\ &= \int_{-\infty}^{\infty} h(x)\overline{\psi_{k,\sigma,\tau}(x)e^{iwx}} dx = \int_{-\infty}^{\infty} \widehat{h}(u)\overline{\mathcal{F}[\psi_{k,\sigma,\tau}(x)e^{iwx}]}(u) du \\ &= \int_{-\sigma}^{\sigma} \widehat{h}(u)\widehat{\psi}_{k,\sigma,\tau}(\omega - u) du. \end{aligned}$$

Here we have used the Parseval equality. Since $\widehat{\psi}_{k,\sigma,\tau}(f)$ is bandlimited of bandwidth $\sigma = c/2\pi$, we have

$$|f - u| \leq \sigma \text{ or } |\omega| \leq |u| + \sigma \leq 2\sigma.$$

Thus, $h(x)\psi_{k,\sigma,\tau}(x) \in \mathbf{B}_{2\sigma}$.

Now we have

$$h_{k,\sigma,\tau} = (h, \psi_{k,\sigma,\tau}) \approx \frac{1}{\lambda_{k,\sigma,\tau}} \sum_{i=1}^n w_i h(x_i)\psi_{k,\sigma,\tau}(x_i). \quad (22)$$

In the rest of the article, we are particularly interested in representation of a digitized signals, that is, signals are given by their discrete samples (usually provided by electronic devices). We further assume that discrete function values are available on $[-\tau, \tau]$, that is, function samples $\{f(-\tau + \frac{\tau k}{2^{M_1-1}})\}_{k=0}^{2^{M_1}}$ are given.

4. Numerical Examples

For any real understanding of the theory, it is necessary to appreciate its numerical aspects. This is true particularly when the available information is given by a discrete set. In this section, we explore properties of Slepian series numerically. These numerical examples are grouped by regularity as we mentioned in the introduction: bandlimited functions, essentially bandlimited functions, analytic functions and functions with jump discontinuity. For simplicity, we take $\tau = 1$. The parameter c_q is related to the bandwidth of the Slepian functions used to construct the quadrature by $\sigma = c_q/2\pi$, that is, we have the following equality,

$$\sum_{k=1}^n \omega_k \psi_{i,c_q,1}(x_k) = \int_{-1}^1 \psi_{i,c_q,1}(x) dx, \quad i = 1, \dots, 2n. \tag{23}$$

We choose $c_q = 10$. The dominate eigenvalue $\lambda_{0,10,1} = 1.000000e+000$, or $\|\psi_{0,10,1}\| = 1.000000e+000$. It is very interesting to note here, the distribution of these quadrature nodes and weights are very well modeled by using cubic spline regression. Figure 4 shows the quadrature nodes, weights and the relation between parameter c and number of nodes. Now we are ready to see numerical examples. It is worth mentioning that the choice of c_q is crucial and tricky. The number of the terms used in the quadrature depends on the choice of c_q . As usual, larger c_q will offer better approximation with higher computing complexity. Figure 6 demonstrates the relation between c_q and the number of terms used in the quadrature. There are 14 pairs of nodes and weights for the generalized Gaussian quadrature when $c_q = 10$ (see Table 1).

4.1. Bandlimited case

Example 4.1 Shannon sampling (sinc) function. The sinc function is given by

$$S(x) = \frac{\sin \pi x}{\pi x} \tag{24}$$

with Fourier transform $\widehat{S}(f) = \chi_{[-1/2,1/2]}$.

Table 1. Quadrature nodes and weights, $c_q = 10$

k	x_k	ω_k	k	x_k	ω_k
1	-9.853939e-001	3.734410e-002	8	1.048325e-001	2.089824e-001
2	-9.242401e-001	8.425565e-002	9	3.103933e-001	2.007597e-001
3	-8.188036e-001	1.254634e-001	10	5.035613e-001	1.841642e-001
4	-6.758728e-001	1.590306e-001	11	6.758728e-001	1.590306e-001
5	-5.035613e-001	1.841642e-001	12	8.188036e-001	1.254634e-001
6	-3.103933e-001	2.007597e-001	13	9.242401e-001	8.425565e-002
7	-1.048325e-001	2.089824e-001	14	9.853939e-001	3.734410e-002

To compute the expansion coefficients (18), we write,

$$S_k = (S, \psi_{k,\sigma,\tau}) = \frac{1}{\lambda_{k,\sigma,\tau}} \int_{-1}^1 S(x) \psi_{k,\sigma,\tau}(x) dx \simeq \sum_{k=1}^{14} \omega_k S(x_k) \psi_{k,\sigma,\tau}(x_k).$$

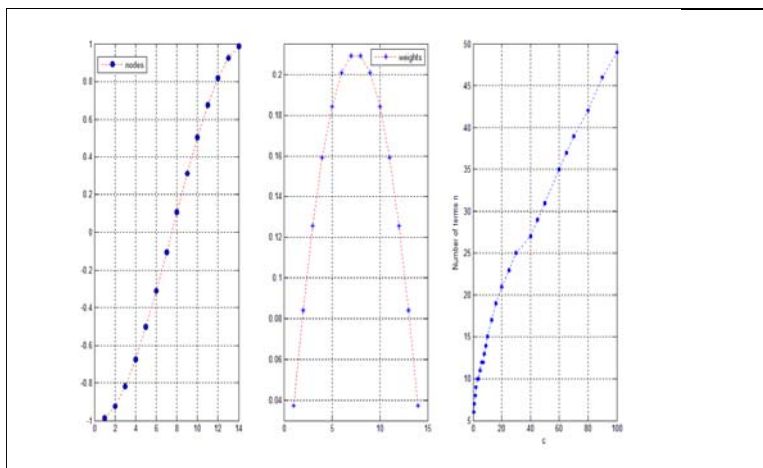


Figure 4. Quadrature nodes (left), weights (meddle) and relation between parameter c and number of nodes, $c_q = 10$.

Notice that the function values $\{S(x_k)\}$ may be not available. In such cases, we used values of the linear interpolating polynomial at nodes $\{S(-1 + \frac{k}{2^{M_1-1}})\}_{k=0}^{2^{M_1}}$ to approximate them. For all examples in this section, we take $M_1 = 7$. That is, there are totally $128+1 = 129$ equally distributed nodes with stepsize $h = 2/2^{M_1} = 2^{-6}$ on interval $[-1, 1]$. These coefficients are then used in the Slepian series expansion (17):

$$S(x) = \sum_{k=0}^{\infty} S_k \psi_{k,\sigma,\tau}(x),$$

which has to be truncated as

$$S_N(x, c) \simeq \sum_{k=0}^{N_c} S_k \psi_{k,c/2\pi,1}(x).$$

The truncation parameter N_c (number of terms in the truncated Slepian series) is dependent on the bandwidth parameter $c = \sigma/2\pi$ of the basis $\psi_{k,c/2\pi,1}$. In Figure 5, we demonstrate the computational result, graphically. Slepian functions with bandwidth π (top), 3π (bottom) are used in the expansion, respectively. The expansion using larger bandwidth has better result.

4.2. Essentially bandlimited case

Example 4.2 Gaussian kernel. Gaussian kernel is defined as, $G(x) = \frac{1}{\sqrt{2\pi}} e^{-\frac{x^2}{2}}$ with Fourier transform given by, $\widehat{G}(w) = e^{-2\pi^2 w^2}$. Notice that the Gaussian kernel is analytic but not exponential type. It is an essentially bandlimited function.

Example 4.3 Bilateral kernel. The bilateral kernel is defined as, $k(x) = e^{-|x|}$, while its Fourier transform is given by, $\widehat{k}(w) = \frac{1}{1+w^2}$. Bilateral kernel is not analytic but exponential type with a corner point at $x = 0$. We observe that its Slepian series has trouble there. See Figure 7 for numerical results.

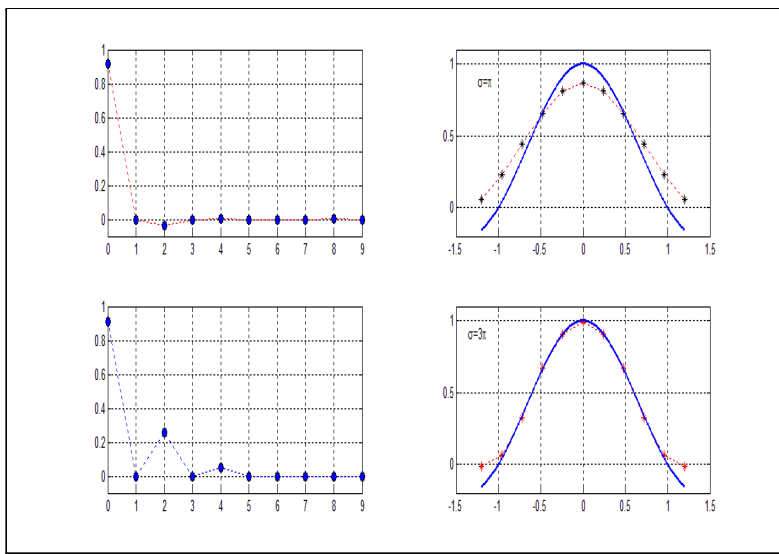


Figure 5. Orthogonal expansion of sinc function (the solid line is the original function). Right: recovered signal. Left: the expansion coefficients.

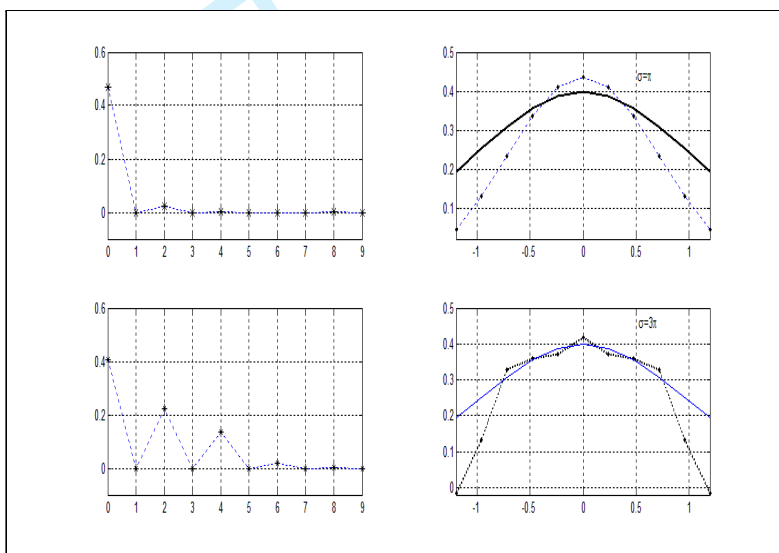


Figure 6. Orthogonal expansion of Gaussian function(solid line is the original function). Right: recovered signal. Left: the expansion coefficients.

4.3. Function with jump discontinuity

Example 4.4 (Function with jump discontinuity). In this example, we consider two functions. The characteristic function of $[-1, 0]$, defined as

$$\chi_{[-1,0]}(x) = \begin{cases} 1, & x \in [-1, 0], \\ 0, & \text{else where.} \end{cases}$$

And the function made up by bilateral kernel $k(x)$, defined by

$$K(x) = \begin{cases} k(x), & x \leq 0, \\ -k(x), & x > 0. \end{cases}$$

Both of these two functions have jump discontinuity at $x = 0$. The expansion coefficients and their associated Slepian series are demonstrated in Figures 9 and

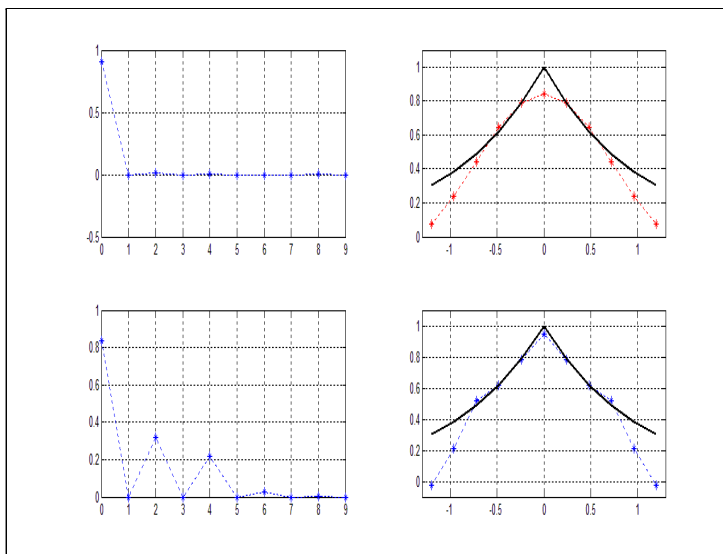


Figure 7. Orthogonal expansion of Bilateral kernel. Right: recovered signal. Left: the expansion coefficients.

10. We observe the slow decay of the coefficients compared to the functions in the previous example. We also notice that the partial sums of their Slepian series are oscillating around the jump discontinuity $x = 0$. The phenomenon is very similar to the Gibbs phenomenon in Fourier series.

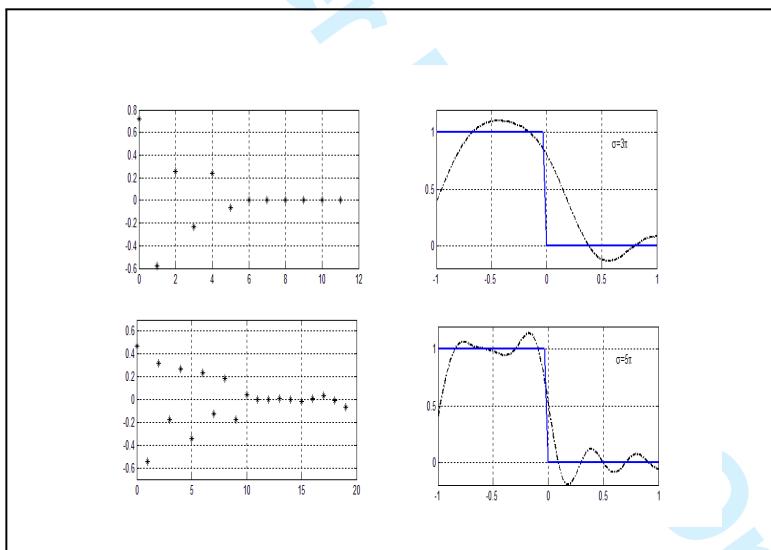


Figure 8. The Slepian series expansion of the characteristic function of $[-1, 0]$ (solid line is the original function) Left: recovered signal. Right: the expansion coefficients.

5. Conclusion

In this article, we demonstrate some numerical results for Slepian series expansion for functions selected from different categories according to their regularity and bandlimits. We observe the following:

1. The convergence rate of the Slepian series is dependent on the regularity and bandlimit of a given signal. It converges rapidly for function in the Paley-

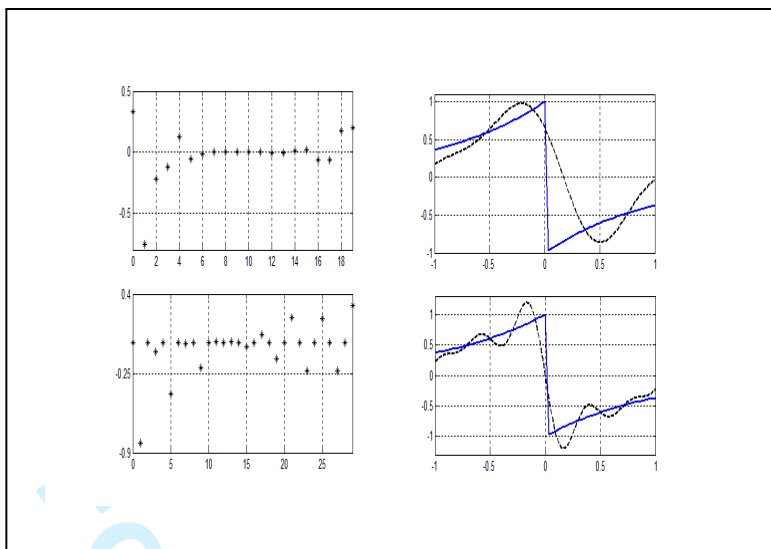


Figure 9. Orthogonal expansion of two pieces of bilateral kernel(solid line is the original function). Left: recovered signal. Right: the expansion coefficients.

Wiener space \mathbf{B}_σ while slower for functions with discontinuity (just like other series expansion).

2. Since Slepian series in this article are derived by using function samples on $[-1, 1]$, their approximation quality degrades outside of the interval $[-1, 1]$ naturally. However, they have relatively good extrapolation properties for functions in \mathbf{B}_σ .

3. Gibbs-like phenomenon is observed for Slepian series when the signals carry jump singularity (see the last two examples).

Other numerical experiments (they will be reported separately) also show that the Slepian series can tolerant noise and work (relatively well with sparsely given function data). Motivated by these observations, we are working on developing a hierarchical system based on Slepian functions and a best-basis type algorithm. It is our hope such a system and an algorithm can be used to represent smooth signals as well as signals with jump discontinuities more effectively.

Acknowledgment

The authors were partially supported by grant ONR YIP N00014-00-1-0469 while completing this paper. They are also in debit to Professors G. Beylkin, V. Rokhlin and H. Xiao for their introducing the Generalized Gaussian quadrature and providing references [1], [36] and [35].

References

- [1] G. Beylkin and L. Monzon, On generalized Gaussian quadratures for exponentials and their applications, *Appl. Comput. Harmon. Anal.* Vol. **12** (2002), No. 3, 332–373.
- [2] C. J. Bouwkamp, On spheroidal wave functions of order zero, *J. Math. Phys.*, **26** (1947), 79-92.
- [3] Ph. Delsarte, A. J. E. M. Janssen, L. B. Vries, Discrete prolate spheroidal wave functions and interpolation. *SIAM Journal on Applied Math.*, Vol. **45** (1985), No. 4, 641-650.
- [4] C. Flammer, *Spheroidal Wave Functions*, Stanford Univ. Press, Stanford, CA, 1956.
- [5] S. Hanish, R. V. Baier, A. L. Van Buren and B. J. King, *Tables of Radial Spheroidal Wave Functions, Volume. 1: Prolate, m = 0*, Tech. Rep. NRL 7088, Naval Research Laboratory, Washington, DC. Available through NTIS, AN: AD723836XAB.
- [6] K. A. Jain, *Fundamentals of Digital Image Processing*, Englewood Cliffs, NJ, Prentice Hall, 1989.
- [7] J. F. Kaiser, *Digital Filter*, Englewood Cliffs, NJ: Prentice-Hall, 1975.
- [8] Kozin, M. B., Volkov, V. V. and D. I. Svergun, A compact algorithm for evaluating linear prolate functions, *IEEE Transactions on Signal Processing*, Vol. **45** (1977), No. 4., 1075-1078.

- 1 [9] D. W. Lozier and F. W. J. Olver, Numerical evaluation of special functions, in *Mathematics of*
- 2 *Computation 1943-1993: A Half-Century of Computational Mathematics*, W. Gautschi, Ed., AMS
- 3 *Proceedings of Symposia in Applied Mathematics*, Vol. **48** (1993), 79-125.
- 4 [10] H. J. Landau and H. Widom, The eigenvalue distribution of time and frequency limiting, *J. Math.*
- 5 *Anal. Appl.* **77** (1980), , 469-481.
- 6 [11] H. J. Landau and H. O. Pollak, Prolate spheroidal wave functions, Fourier analysis and uncertainty-II,
- 7 *Bell System Tech J.* **40** (1961) 65-84.
- 8 [12] H. J. Landau and H. O. Pollak, Prolate spheroidal wave functions, Fourier analysis and uncertainty-
- 9 III: The dimension of the space of essentially time- and band-limited signals, *Bell System Tech J.* **41**
- 10 (1962), 1295-1336.
- 11 [13] A. Papoulis, *Signal Analysis*, McGraw-Hill, New York, 1977.
- 12 [14] W. Rudin, *Functional Analysis*, McGraw-Hill, New York, 1973.
- 13 [15] C. E. Shannon, Communication in the presence of noise, *Proc. IRE* **37** (1949), 10-21.
- 14 [16] X. Shen and N. Saito, Recovering piecewise band-limited signals via a hierarchical system based on
- 15 prolate spheroidal wave functions, AMS annual meeting #983, January 2003, Baltimore, Maryland.
- 16 [17] X. Shen and G. G. Walter, Construction of periodic prolate spheroidal wavelets using interpolation.
- 17 Vol. 40 (2007) No. 3-4, 445-466.
- 18 [18] L. Shepp and C.-H. Zhang, Fast Functional Magnetic Resonance Imaging via Prolate Wavelets, Ap-
- 19 plied and Computational Harmonic Analysis Vol. 9 (2000), 99-119.
- 20 [19] D. Slepian, Some comments on Fourier analysis, uncertainty, and modeling, *SIAM Review* **25** (1983),
- 21 379-393.
- 22 [20] D. Slepian, Prolate spheroidal wave functions, Fourier analysis and uncertainty-V: The discrete case,
- 23 *Bell System Tech J.* **57** (1978), No. 5, 3009-3058.
- 24 [21] D. Slepian, A numerical method for determining the eigenvalues and eigenfunctions of analytic kernels.
- 25 *SIAM J. Numer. Anal.* **5** (1968) 586-600.
- 26 [22] D. Slepian, Prolate spheroidal wave functions, Fourier analysis and uncertainty-IV: Extensions to
- 27 many dimensions, generalized prolate spheroidal functions, *Bell System Tech J.* **43** (1964), 3009-
- 28 3058.
- 29 [23] D. Slepian, H. O. Pollak, Prolate spheroidal wave functions, Fourier analysis and uncertainty-I, *Bell*
- 30 *System Tech J.* **40** (1961), 43-64.
- 31 [24] D. Slepian, Some asymptotic expansions for prolate spheroidal wave functions, *J. Math. Phys.* **44**
- 32 (1965) 99-140.
- 33 [25] F. Stenger, *Numerical Methods Based On Sinc And Analytic Functions*, Springer-Verlag, New York,
- 34 (1993).
- 35 [26] A. H. Stroud and D. Secrest, *Gaussian Quadrature Formulas*, Englewood Cliffs, N.J., Prentice-Hall
- 36 (1966).
- 37 [27] A. L. Van Buren, B. J. King and R. V. Baier, Tables of angular spheroidal wave functions, Vol. 1:
- 38 Prolate, $m = 0$, Tech. Rep., Naval Research Laboratory, Washington, DC. Available through NTIS,
- 39 1975.
- 40 [28] A. L. Van Buren, A Fortran computer program for calculating the linear prolate functions, Tech. Rep.
- 41 NRL 7994, Naval Research Laboratory, Washington, DC. Available through NTIS, 1976.
- 42 [29] G. G. Walter, Differential operators which commute with characteristic functions with applications
- 43 to a lucky accident, *Complex Variables Vol.* **18** (1992), 7-12.
- 44 [30] G. G. Walter, Prolate spheroidal wavelets: translation, convolution, and differentiation made easy. *J.*
- 45 *Fourier Anal. Appl.* **11** (2005), No. 1, 73-84.
- 46 [31] G. G. Walter and X. Shen, Wavelets based on prolate spheroidal wave functions, *Journal of Fourier*
- 47 *Analysis and Applications*, Vol. **10**, (2004), No.1, 1-26.
- 48 [32] G. G. Walter and X. Shen, Sampling with prolate spheroidal wave functions, *J. Sampling Theor.*
- 49 *Signal Image Process.* Vol. **2** (2003) 25-52.
- 50 [33] R. Wilson, Finite prolate spheroidal sequences and their applications I: Generation and properties,
- 51 *IEEE Transactions on Pattern Analysis and Machine Intelligence*, Vol. **9** (1987), No. 6, 787-795.
- 52 [34] R. Wilson R. and M. Span, Finite prolate spheroidal sequences and their applications II: Image feature
- 53 sescription and segmentation, *IEEE Transactions on Pattern Analysis and Machine Intelligence*, Vol.
- 54 **10** (1988), No. 2, 193-203.
- 55 [35] H. Xiao, *Prolate Spheroidal Wave Functions, Quadrature, Interpolation, and Asymptotic Formulae*,
- 56 Ph.D thesis, Yale University, 2001.
- 57 [36] H. Xiao, V. Rokhlin and N. Yarvin, Prolate spheroidal wavefunctions, quadrature and interpolation,
- 58 *Inverse Problems Vol.* **17** (2001), No. 4, 805-838.
- 59 [37] S. Zhang, J.M. Jin, *Computation of Special Functions*, Wiley, New York, 1996.
- 60 [38] A. I. Zayed, *Handbook of Function and Generalized Function Transformations*, Mathematical Sciences
- Reference Series, Vol. **3** (1996), CRC Press, Boca Raton, FL.

1
2
3
4
5
6
7
8
9
10
11
12
13
14
15
16
17
18
19
20
21
22
23
24
25
26
27
28
29
30
31
32
33
34
35
36
37
38
39
40
41
42
43
44
45
46
47
48
49
50
51
52
53
54
55
56
57
58
59
60

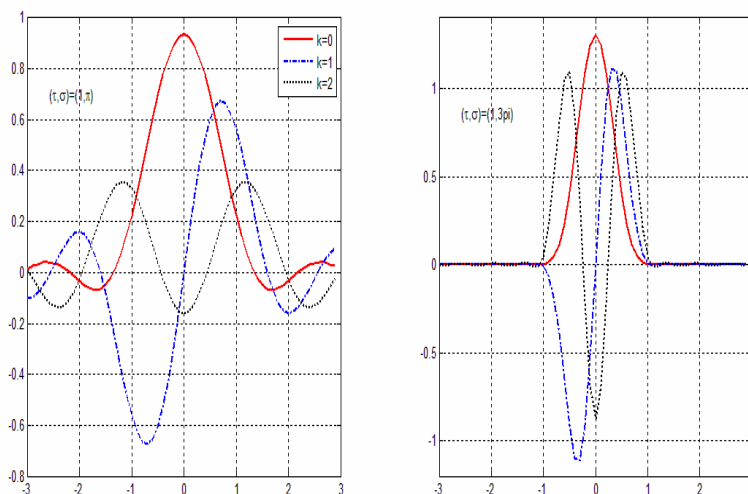


Figure 1. Slepian functions $\psi_{n,\sigma,\tau}$. Top panel: $(\tau, \sigma) = (1, \pi)$, $n=0, 1, 2$. Bottom panel: $(\tau, \sigma) = (1, 3\pi)$, $n=0, 1, 2$.

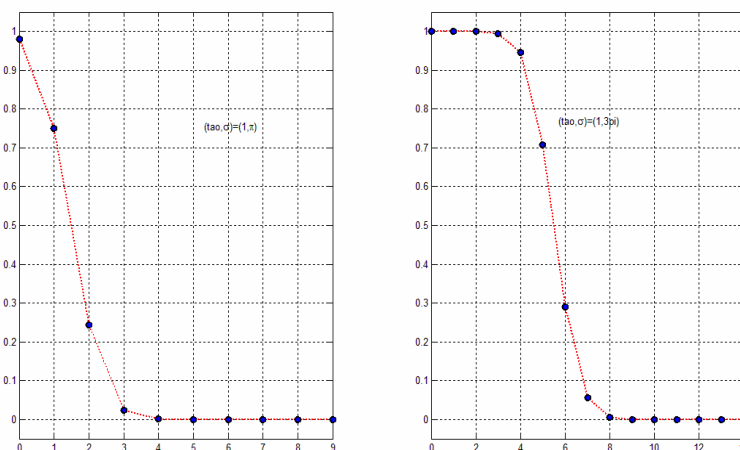


Figure 2. Associated eigenvalues $\lambda_{n,\sigma,\tau}$. Left panel: $(\tau, \sigma) = (1, \pi)$, $n=0, 1, 2, \dots, 9$. Right panel: $(\tau, \sigma) = (1, 3\pi)$, $n=0, 1, 2, \dots, 14$.

1
2
3
4
5
6
7
8
9
10
11
12
13
14
15
16
17
18
19
20
21
22
23
24
25
26
27
28
29
30
31
32
33
34
35
36
37
38
39
40
41
42
43
44
45
46
47
48
49
50
51
52
53
54
55
56
57
58
59
60

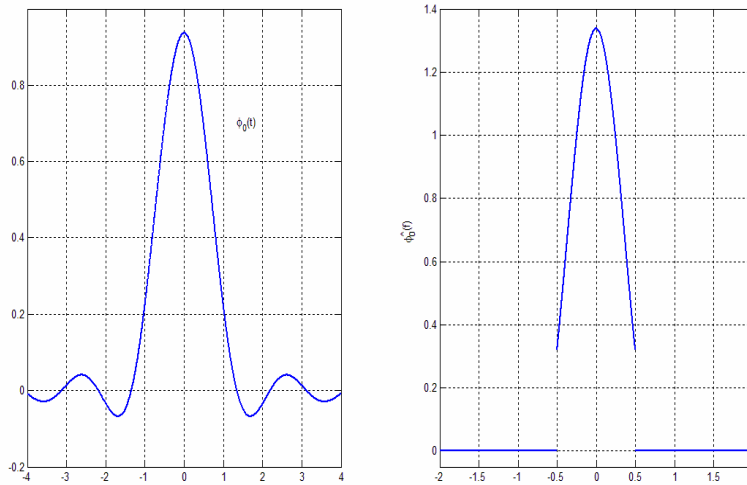


Figure 3. Slepian function $\psi_{0,\pi,1}(x)$ (top panel) and its Fourier transform $\tilde{\psi}_{0,\pi,1}(\omega)$ (bottom panel).

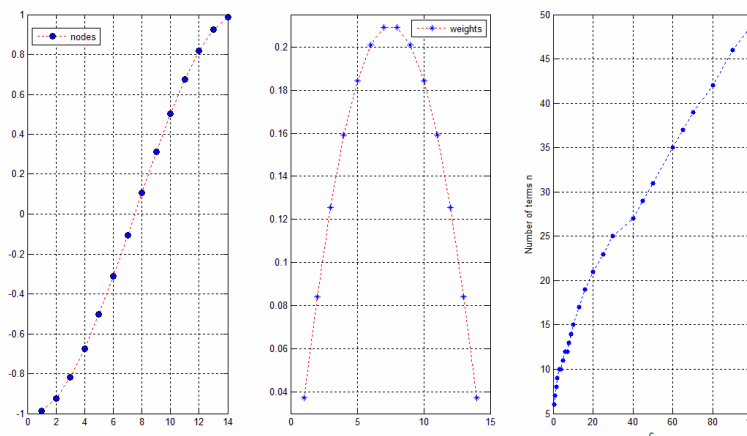


Figure 4. Quadrature nodes (left), weights (middle), $c_q = 10$ and relation between parameter c and number of nodes (right), $c_q = 10$.

1
2
3
4
5
6
7
8
9
10
11
12
13
14
15
16
17
18
19
20
21
22
23
24
25
26
27
28
29
30
31
32
33
34
35
36
37
38
39
40
41
42
43
44
45
46
47
48
49
50
51
52
53
54
55
56
57
58
59
60

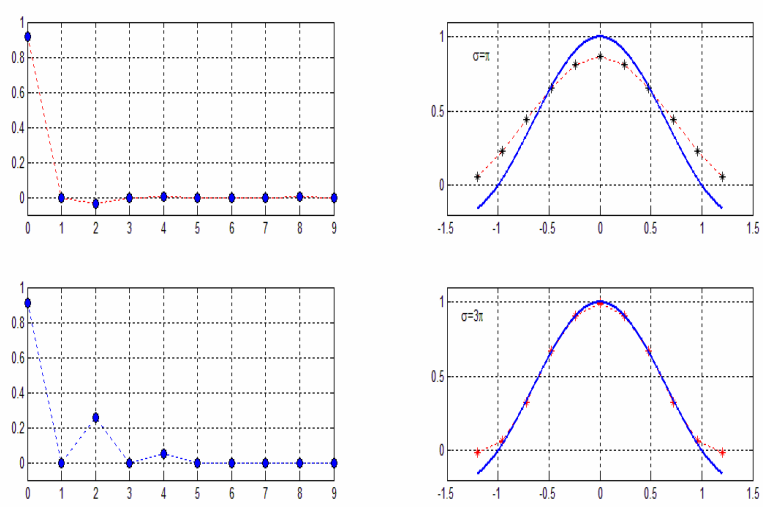


Figure 5. Orthogonal expansion of sinc function (the solid line is the original function). Right: recovered signal. Left: the expansion coefficients.

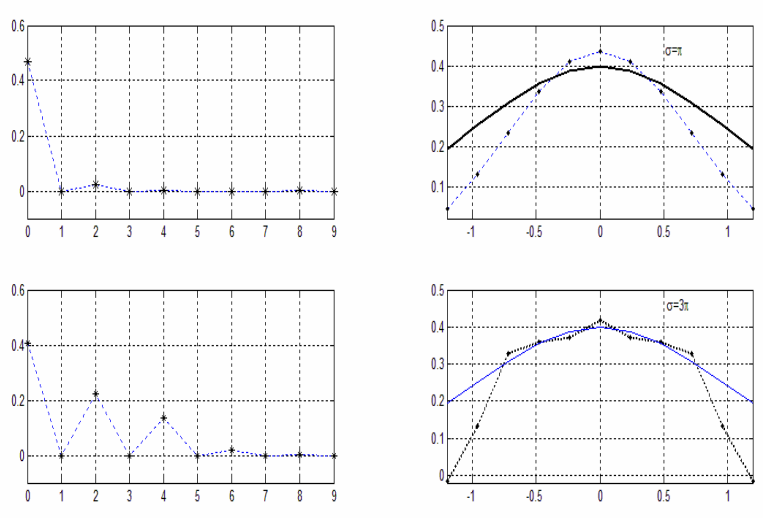


Figure 6. Orthogonal expansion of Gaussian function (solid line is the original function). Right: recovered signal. Left: the expansion coefficients.

1
2
3
4
5
6
7
8
9
10
11
12
13
14
15
16
17
18
19
20
21
22
23
24
25
26
27
28
29
30
31
32
33
34
35
36
37
38
39
40
41
42
43
44
45
46
47
48
49
50
51
52
53
54
55
56
57
58
59
60

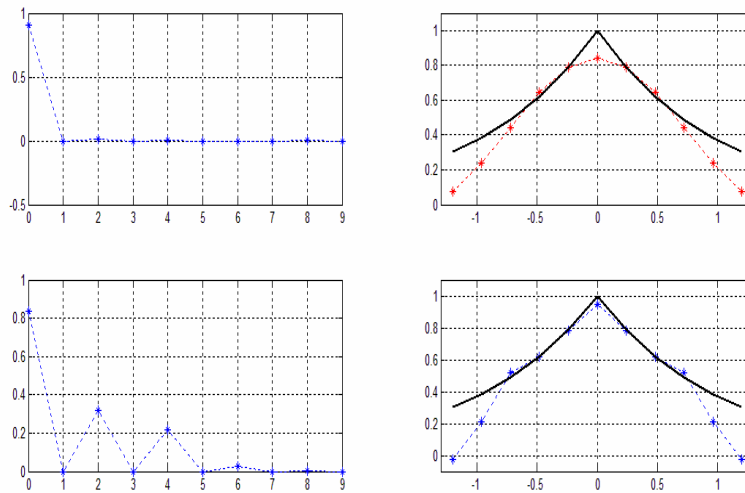


Figure 7. Orthogonal expansion of Bilateral kernel (solid line is the original function). Right: recovered signal. Left: the expansion coefficients.

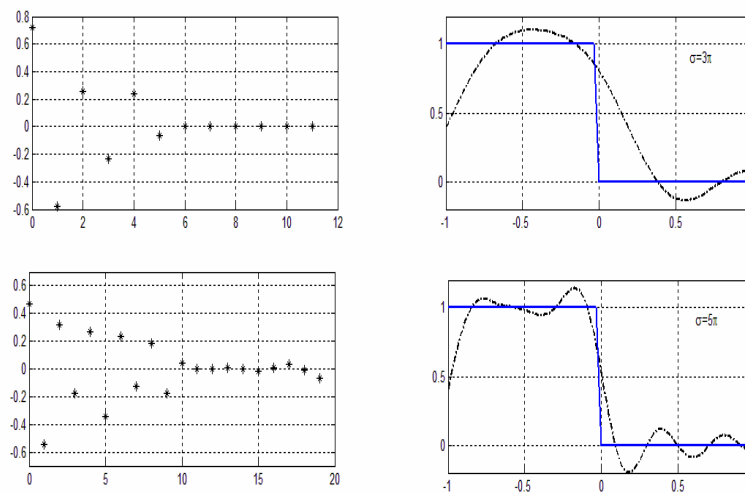


Figure 8. The Slepian series expansion of the characteristic function of $[-1, 0]$ (solid line is the original function). Left: recovered signal. Right: the expansion coefficients.

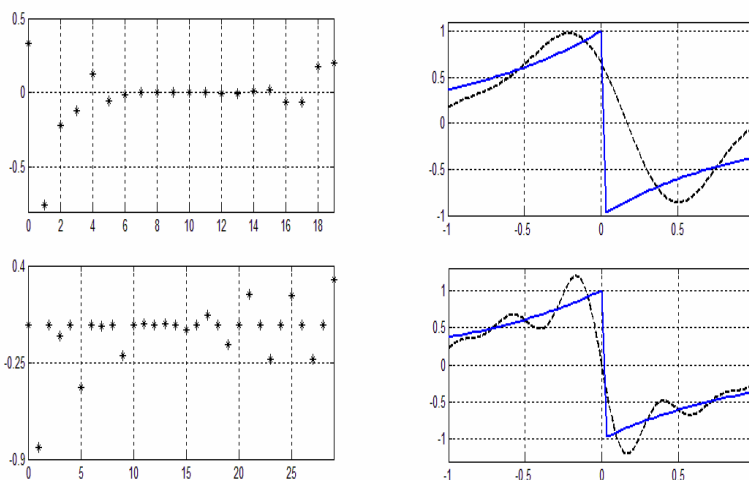


Figure 9. Orthogonal expansion of two pieces of bilateral kernel. Left: recovered signal (solid line is the original function). Right: the expansion coefficients.

Table 1. Quadrature nodes and weights, $c_q = 10$

k	$x_{\{k\}}$	$\omega_{\{k\}}$	k	$x_{\{k\}}$	$\omega_{\{k\}}$
1	-9.853939e-001	3.734410e-002	8	1.048325e-001	2.089824e-001
2	-9.242401e-001	8.425565e-002	9	3.103933e-001	2.007597e-001
3	-8.188036e-001	1.254634e-001	10	5.035613e-001	1.841642e-001
4	-6.758728e-001	1.590306e-001	11	6.758728e-001	1.590306e-001
5	-5.035613e-001	1.841642e-001	12	8.188036e-001	1.254634e-001
6	-3.103933e-001	2.007597e-001	13	9.242401e-001	8.425565e-002
7	-1.048325e-001	2.089824e-001	14	9.853939e-001	3.734410e-002